Available online at www.sciencedirect.com

SciVerse ScienceDirect

Russian Geology and Geophysics 53 (2012) 185–193

RUSSIAN GEOLOGY AND GEOPHYSICS

www.elsevier.com/locate/rgg

The geoelectric structure at the site of "Crystal" underground nuclear explosion (*Western Yakutia*) from TEM data

N.O. Kozhevnikov [a,*], E.Yu. Antonov [a], S.Yu. Artamonova [b], A.E. Plotnikov [c]

[a] *A.A. Trofimuk Institute of Petroleum Geology and Geophysics, Siberian Branch of the Russian Academy of Sciences, pr. Akademika Koptyuga 3, Novosibirsk, 630090, Russia*

[b] *V.S. Sobolev Institute of Geology and Mineralogy, Siberian Branch of the Russian Academy of Sciences, pr. Akademika Koptyuga 3, Novosibirsk, 630090, Russia*

[c] *LUCH R&D Company for Geophysical Instruments, ul. Geologicheskaya 49, Novosibirsk, 630010, Russia*

Received 25 May 2010; accepted 7 October 2010

Abstract

The resistivity pattern at the site of the "Crystal" underground nuclear explosion (Daldyn–Alakit district of Yakutia) of 1974 which led to an accident has been imaged using TEM data. The local background pattern corresponds to a three- or four-layer earth with a conductor at the base. The uppermost layer, with a resistivity of tens to hundreds of ohm · m, has its bottom at 190–260 m asl and consists of perennially frozen Late Cambrian carbonates. The resistivity structure of shallow subsurface at the blast epicenter remained unperturbed though being subject to mechanic and thermal effects. The bottom of the second layer is at 20 to 190 m below the sealevel and its resistivity is 7–10 ohm · m. It is composed of frost-bound and unfrozen cold rocks that belong to a Late Cambrian water-bearing sequence (an aquifer). The third and fourth layers make up the conducting base of the section (0.2–1.4 ohm · m) while the conductor's top matches the table of a Middle Cambrian aquifer. Anomalous transient response at the site prompts the existence of a local conductor possibly produced by highly saline waters in the containment cavity and in deformed rocks around it. However, the resistivity is too low (0.02 ohm · m) to be accounted for by any model available at the present state of knowledge. Another problem is to explain how the brines circulating at large depths may have reached the explosion cavity and the surrounding strained zones. The study has provided a first idea of the background resistivity distribution and its UNE-induced changes.

Keywords: underground nuclear explosion (UNE); environment; groundwater; permafrost; radionuclides; TEM surveys; petrophysics; Yakutia

Introduction

The 1.7 kt contained thermonuclear explosion "Kristall" (*Crystal*) for ground swelling, the first one in the USSR, was conducted on October 2, 1974 in the Daldyn–Alakit district of Yakutia, 3.5 km northeast of the Udachnaya kimberlite pipe, near the Ulakhan-Bysyttakh inlet into the Daldyn River (Fig. 1, *a*) (Golubov et al., 2004). The charge was placed in a borehole at a depth of 98 m below the surface in fractured frozen Late Cambrian carbonate sediments. The project stipulated blasting at seven more points along a profile in order to build a swell dam for a tailing dump at the Udachny mining-and-concetrator combine. The ground swell was supposed to dam the Ulakhan-Bysyttakh Creek and to be 1800 m long, 27–30 m high, and 85 m wide at the crest. The ejected ground reached the maximum height of 60 m at the fourth second after detonation, then settled down and produced a bank, only 14 m high, i.e., twice lower than it was expected. Furthermore, the fissure products were released into air in a radionuclide cloud over a strip of several kilometers long directed at 70°. As a result, the explosion was considered to be an accident and further blasting was cancelled. The Udachny combine changed the place of the tailing dump and refused the UNE technologies (Golubov et al., 2004; Yablokov, 2009).

After 1990 a number of research and development institutions investigated the fallout from the "Crystal" explosion, but mostly within specific landscape elements of the area (soils, rivers and lakes, groundwater, etc.). Those studies overlooked subsurface groundwater transport of radionuclides through rocks deformed by the blast. Meanwhile, underground nuclear explosions are the most powerful of manmade agents disturbing the subsurface (Mikulenko et al., 2004; Yablokov, 2009),

* Corresponding author.
E-mail address: KozhevnikovNO@ipgg.nsc.ru (N.O. Kozhevnikov)

1068-7971/$ - see front matter © 2012, V.S. Sobolev IGM, Siberian Branch of the RAS. Published by Elsevier B.V. All rights reserved.
doi:10.1016/j.rgg.2011.12.015

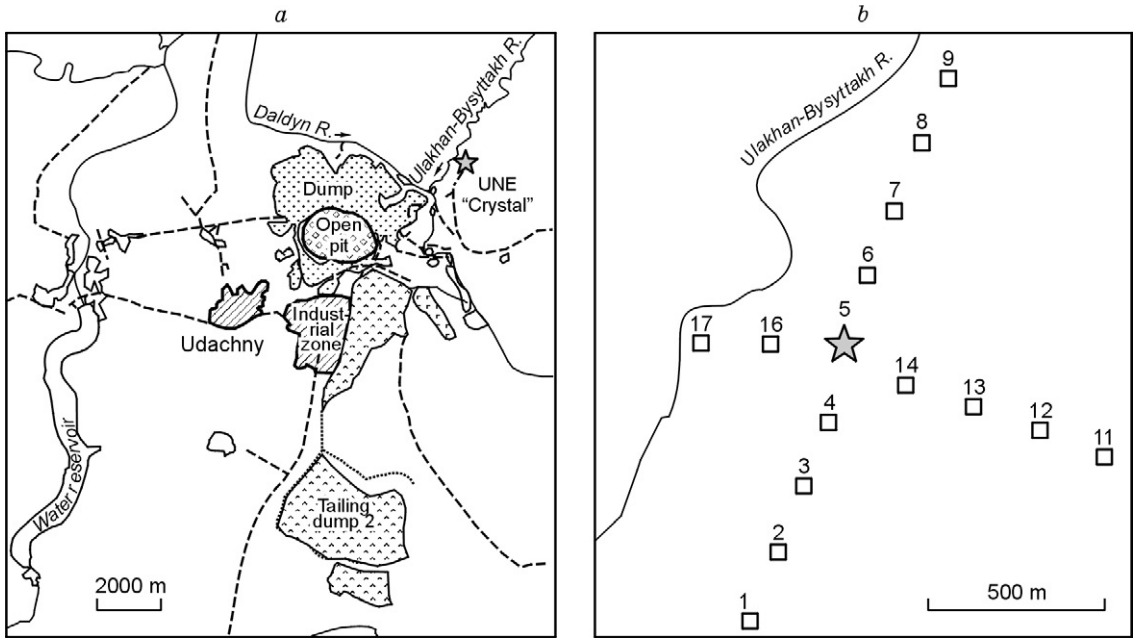

Fig. 1. Location map of "Crystal" underground nuclear explosion near Udachny town (*a*) and TEM stations (*b*).

and they are these changes that should be the main focus of research (Burtsev et al., 2004).

According to ample evidence from different regions of Russia, borehole nuclear blasts can change the state and composition of both bedrock and thick unconsolidated sediments in shallow subsurface (Mel'nikov et al., 2000; Stognii, 2004).

The case of "Crystal" is especially serious as it was detonated in permafrost, unlike many other tests of this kind. One may expect that such a powerful thermal and tectonic event interferes with the permafrost setting and perturbs the environment and its thermal equilibrium. UNE in the permafrost zone have an important consequence of soil heating associated with activity of fluid systems, including groundwater circulation along vertical fractured zones (Stognii, 2004).

Geological background

The "Crystal" explosion site is located in the eastern flank of the Tunguska basin (Siberian craton) in Late Cambrian carbonates of the Morkoka Formation (Golubov et al., 2004; Mikulenko et al., 2006). The Morkoka Formation stripped by borehole No. 1E ("Crystal" UNE) lies under 0–5 m of unconsolidated Quaternary sediments (loam, gravel, pebble, and debris) and consists of jointed marl (at 5 to 9.8 m), weakly jointed limestone (9.8–21.5 m), and alternated limestone-marl layers (21.5–106 m).

Permafrost at the site consists of three layers (Alekseev, 2009; Drozdov, 2006; Klimovsky and Gotovtsev, 1994), with ice-rich rocks above (ice filling pores, cracks, and cavities), unfrozen cold rocks with cryopeg lenses (frozen saline water and brines filling voids) below, and frost-bound rocks in-between.

The ground beneath permafrost is saturated with saline waters and is a system of Neoproterozoic and Cambrian aquifers which may be interconnected through permeable zones of faults in sediments or in kimberlites.

The groundwater salinities (TDS) increase progressively with depth being in the ranges from fractions of g/l to 12 g/l in fresh and brackish waters (ice) in the upper layer; 30 to 250 g/l in saline waters and brines of the second layer, and up to 400 g/l in strong and very strong brines below the permafrost (Alekseev, 2009).

Choice of methods

Surface geophysical surveys are obviously the most advantageous tool to study effects of underground nuclear explosions on the subsurface as they provide 3D images of rocks *in situ*. Furthermore, geophysical methods are nondestructive, relatively cheap, and allow depth and resolution monitoring while the soundings.

Note, however, that the engineering geological, geocryological, and other parameters of the section inferred from geophysical data may bear significant errors because of high lateral variability, even if checked against sampling from boreholes and/or mines at the same site. Unlike the logging methods employed in boreholes or mines, surface geophysical data represent a generalized characteristic of large rock masses.

As we have found out, the published evidence on UNE effects on the environment is scanty and mostly restricted to seismic methods. Publications dealing with geophysical measurements for the state of permafrost are very few. There was a study by Stognii (2004) but the measurements were too

shallow to make a basis for 3D mapping of rocks in a UNE area.

The "Crystal" site, with its local geology, permafrost, and groundwater settings is well suitable for TEM soundings. The background section (undisturbed by UNE) in the area consists of distinct almost horizontal resistivity layers that record vertical temperature zoning and saturation with highly saline waters. Near-field TEM measurements are especially efficient as they allow precise estimates of depths to conductors' upper (due to *H* equivalence (Matveev, 1974)) and lower (for thick conductors (Rabinovich, 1987)) boundaries. One may reasonably expect that UNE-induced changes to the position of aquifers would show up in transients. On the other hand, the containment cavity and cracks produced by the explosion and filled with saline waters may appear as local conductors embedded into the background section. TEM soundings can successfully resolve and characterize such conductors, e.g., in mineral exploration practice (Vakhromeev and Kozhevnikov, 1988), and have an additional advantage of going without galvanic earthing when applied to permafrost.

Therefore, the TEM method was chosen to study the site of the "Crystal" explosion. The method has been well developed, especially due to V.A. Sidorov, G.A. Isaev, and other Russian geophysicists who have synthesized the theory, modeling approaches, and techniques of data acquisition and processing.

TEM data were collected along two orthogonal profiles that crossed the explosion epicenter (point 5, Fig. 1, *b*). N–S profile 1 (points 1–9) was oriented along the azimuth 16°, and W–E profile 2 (points 11–17) consisted of two segments with different orientations: a shorter one (5, 16, 17) at the azimuth 83° and a longer one (11–14) at 103°. The results of the experiment were reported earlier at the 3rd International Conference "Radioactivity and Radioactive Elements in the Human Environment" in Tomsk and at the 6th Russian Workshop "Radiochemistry-2009" in Moscow (Artamonova et al., 2009a,b).

Methods of field measurements

The TEM data acquisition was in the classical way (Vanchugov and Kozhevnikov, 1998), with a square central-loop configuration and the measurement points at the loop center. The transmitter and receiver loops were, respectively, 6 mm^2 and 1 mm^2 copper wires of the sizes 100 by 100 m and 50 by 50 m. The loop size and spacing were selected proceeding from general considerations for the lack of *a priori* information on the local resistivity structure. Sampling was at every 200 m on average, in accordance with the wanted penetration depth.

The measurement system *SGS-TEM* included several units: (1) a laptop and a telecommunication adapter; (2) a *US-2* synchronizer and ampermeter; (3) two telemeters *Piket-2* units for measuring voltage $e(t)$ in the receiver loop and current I in the transmitter; 31 μs time sampling interval provided high resolution. The data at each sounding point were averaged over a time series of 100 transients, with no less than 10 measurements at each point. Thus, at least 1000 responses were measured in total at each point, which improved the signal/noise ratio by a factor of 30 or better.

Transmitter current was generated by a system, designed at the *Luch* Company, which emitted up to 40 A discrete transient pulses at different periods depending on the duration of the transient response.

The transmitter was powered by 12–24 V acid batteries and had an amperage from 1.7 to 7.5 A. Even that low amperage was enough to measure transients at times about 100–150 ms and penetrate to 400–500 m depths due to the absence of industrial noise in the area.

The earliest time t_{min}, known (Kozhevnikov and Plotnikov, 2004) to define the minimum penetration depth, was 0.2 ms on average and depended more on the time when the transmitter current was turned off rather than on the resistivity of the ground.

Presentation of TEM data

TEM soundings measure voltage in the receiver loop normalized to the transmitter current (normalized response) but the data are commonly analyzed and interpreted using the parameter of apparent resistivity (ρ_a, ohm · m):

$$\rho_a = \left[\frac{I S_t S_r}{e(t) 20\pi\sqrt{\pi}}\right]^{2/3} \left(\frac{\mu_0}{t}\right)^{5/3},$$

where t is the time in seconds; S_t and S_r are, respectively, the surface areas of the transmitter and receiver loops, m^2; $e(t)$ is the voltage induced in the receiver, V; I is the transmitter current, A; $\mu_0 = 4\pi \times 10^{-7}$ H/m (Kaufman and Morozova, 1970).

The time dependences of apparent resistivity measured at some point (apparent resistivity or ρ_a curves) show how the apparent (and also true, to a certain degree) resistivity changes with depth. Lateral ρ_a variations are imaged by plotting ρ_a in 1D (profiles) at certain fixed times.

Effective depth is a parameter used at the preliminary stage of data imaging. It corresponds to skin depth in the frequency domain and is given by

$$H_{ef} = k\sqrt{t\rho_a(t)}, \quad (1)$$

where H_{ef} is the effective depth, m; k is the constant; t is the time, s; and $\rho_a(t)$ is the apparent resistivity, ohm · m. Taking into account the previous experience of TEM data processing, H_{ef} were calculated assuming k = 500–800 (Vakhromeev and Kozhevnikov, 1988).

Inversion of TEM data was performed within the limits of a layered-earth model using the <Unv_QQ> and <Inv_QQ> software (designed by E.Yu. Antonov, Institute of Petroleum Geology and Geophysics, Novosibirsk). Figure 2 illustrates the inversion quality: typical measured and computed apparent resistivity curves are shown in the left panel and the corre-

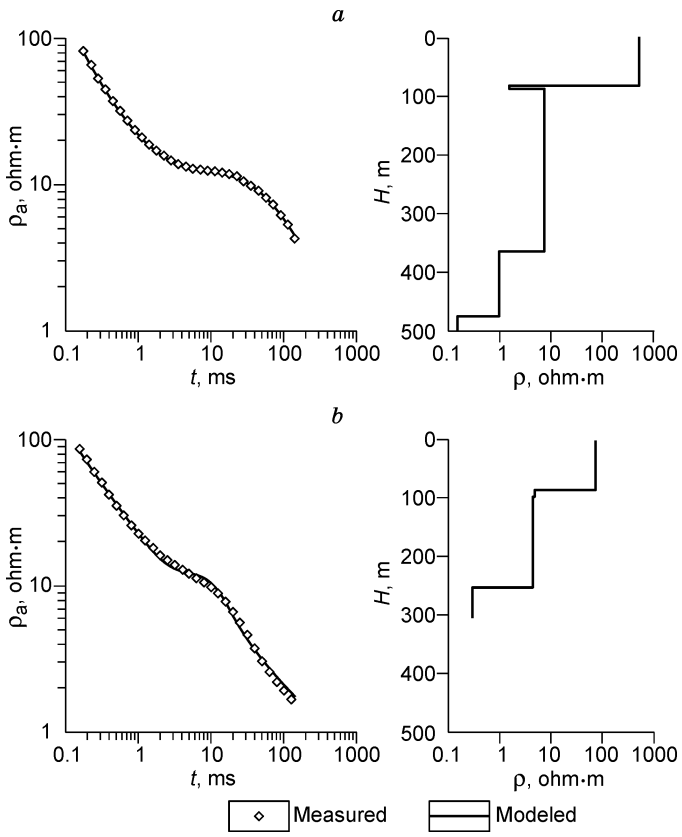

Fig. 2. Apparent resistivity curves (left panel) and models (right panel): *a*, away from UNE epicenter; *b*, at UNE epicenter (point 5).

sponding models are in the right panel, with the rms errors 2% and 6%, respectively (Fig. 2, *a*, *b*).

Results

Profile 1. Almost all ρ_a curves measured along profile 1 (Fig. 3, *a*) coincide with one another which is evidence of a uniform resistivity pattern within the survey area. Most of the curves are of Q-, HQ- or QQ-types. The ρ_a curves measured at point 5 (explosion epicenter) and at point 6 stand out against the others and may be classified as anomalous, especially those at point 5. Note that the response at point 5 is the same as elsewhere at early times ($t < 3$ ms), i.e., the resistivity of the shallowest subsurface at the UNE epicenter does not differ from that in other parts of the profile, but it decreases progressively with depth. At point 6, ρ_a is slightly lower at early times and slightly higher at intermediate times relatively to the background curves; at late times it coincides with the background.

Figure 4, *a* shows ρ_a plots along the N–S profile (for fixed times). According to equation (1), each subsequent plot in Fig. 4, *a* represents the resistivity to a depth about twice as great as the previous one. Apparent resistivities in the profile flanks remain the same at any time and are parallel to the *x*-axis at early times ($t \le 3.2$ ms), the latter being evidence of a uniform shallow structure. At point 6, ρ_a are slightly below the background at 0.2 and 0.8 ms but are notably lower at late times ($t \ge 12.5$ ms) in the central segment of the profile. Therefore, the anomaly-producing object must be rather deep.

These inferences agree with 1D inversion results (Fig. 4, *b*, *c*). Apparent resistivity decreases with depth at each point. The upper layer has the thickness h_1 from 70 to 130 m and the resistivity ρ_1 from 50 to 120 ohm · m, increasing generally in the southern direction. Below there lies another layer with ρ_2 from 7.5 to 9 ohm · m and h_2 = 300–360 m (except for point 5 where $h_2 \approx 150$ m and ρ_2 = 4.4 ohm · m). Then there follows the third layer which may be interpreted as the section base at the reached sounding depth. It has the resistivity ρ_3 = 0.5–1.4 ohm · m and the depth to its top is 350 to 450 m, decreasing, respectively, to ρ_3 = 0.3 ohm · m and 250 m at the explosion epicenter.

Profile 2. All transients along profile 2, except that at point 5 (Fig. 3, *b*) are more or less the same at early times (t < 10 ms). Like the case of profile 1, ρ_a at the UNE epicenter (point 5) is anomalously low at late times. Thus, conducting rocks lie at shallower depths in the profile center than on the flanks along the W–E profile as well.

The same regularity shows up in profiling data (Fig. 5, *a*): the resistivity ρ_a increases from the western flank to the eastern one and no local anomalies appear at the times t = 0.2–3.2 ms, but it decreases markedly at the epicenter at late times ($t \ge 12.5$ ms).

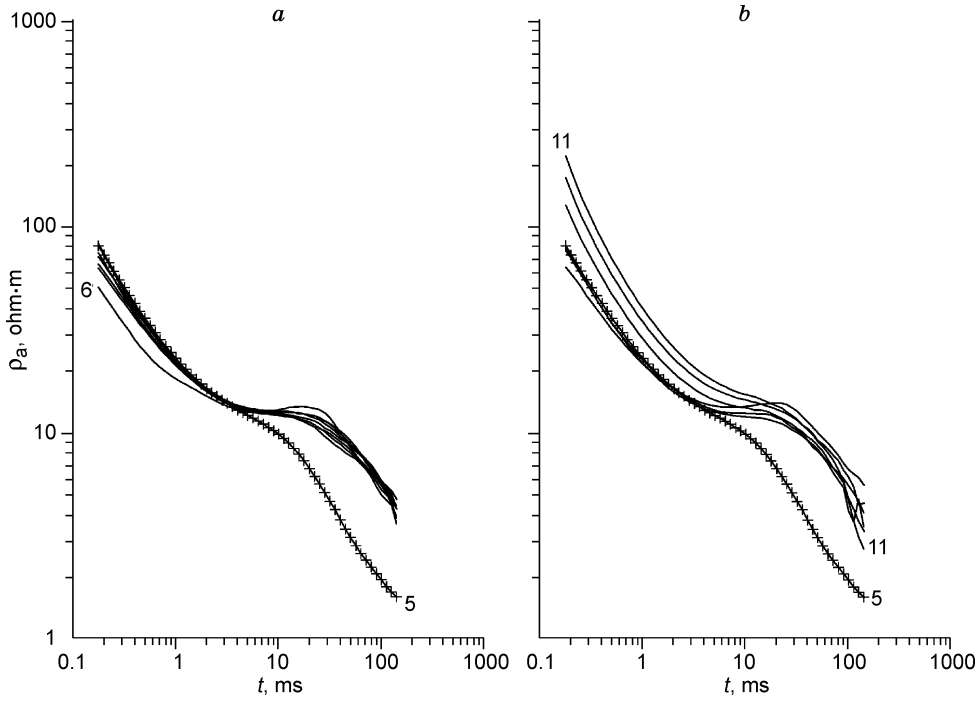

Fig. 3. Apparent resistivities (ρ_a) measured along N–S (*a*) and W–E (*b*) profiles. Numerals near the curves correspond to numbers of TEM data points in Fig. 1, *b*.

The quantitative estimates obtained through inversion (Fig. 5, *b*, *c*) show a progressive depthward resistivity decrease with depth, in the same way as on the N–S profile: ρ_1 = 50–700 ohm · m, ρ_2 = 4.4–10 ohm · m, and ρ_3 = 0.7–1.4 ohm · m. The top of the second layer lies at the depth 80–130 m and that of the third layer is at 440 to 500 m, but is as shallow as 250 m at point 5, i.e., the uplift is no less than 200 m.

As we have mentioned, the descending right branches of ρ_a curves along both profiles indicate the presence of a deep conductor. The apparent resistivity curves correspond to Q-type in most cases.

The latest-time (t > 100 ms) data were considered unreliable and were not used in the inversion. When those transients were included, inversion led to a QQ-type model, with a boundary in the southern flank of profile 1 (points 2–4) at a depth about 450 m below which the resistivity decreased to 0.16–0.4 ohm · m (Fig. 4, *c*).

Transients from about a half of points record a thin conducting layer (~4 S) between the upper and lower layers, i.e., at a depth about 100 m (Figs. 3, *a*, 4, *a*, *b*), which further improves the inversion quality (fit between measured and computed responses).

Discussion

The background resistivity pattern generally corresponds to a Q- ($\rho_1 > \rho_2 > \rho_3$) or, possibly, QQ-type ($\rho_1 > \rho_2 > \rho_3 > \rho_4$) layered earth with resistivities from tens to hundreds of ohm · m and 7 to 10 ohm · m in the first (upper) and second layers, respectively; the third (lower) layer has a resistivity in the range 0.4–1.4 ohm · m (from 0.2 ohm · m at points where the QQ model can apply). Thus, the resistivity of the second layer is one or two orders of magnitude lower than that of the upper one and the conducting base is an order of magnitude (or more) less resistive than the second layer. The upper layer is uniform in thickness and lacks local resistivity anomalies. Its bottom (and, correspondingly, the top of the second layer) is almost horizontal. The response from the UNE epicenter is anomalous: the apparent resistivity at point 5 is nearly 10 times lower than at other points at t > 10 ms. 1D inversion images the anomaly as a 200–250 m swell of the lower layer.

Below we are trying to interpret the obtained patterns in terms of a reasonable petrophysical model taking into account the available geological, hydrogeological, and geocryological evidence (Alekseev, 2009; Mikulenko et al., 2006).

The upper layer has average thicknesses (h_1) of 80 and 110 m along profiles 1 and 2, respectively, and is the most resistive. It is permafrost according to cryological data. The ρ_1 values along profile 2 grow eastward to reach 200–700 ohm · m on the eastern flank. The available knowledge being insufficient to account for this trend, we may only tentatively attribute it to variations in ice and/or clay contents in the Morkoka Formation.

The resistivity of the second layer (ρ_2) is within a narrow range of 7 to 10 ohm · m but is as low as 4.4 ohm · m at point 5. The layer's depth interval corresponds to frost-bound or unfrozen Late Cambrian rocks and a subpermafrost aquifer with saline and brackish waters. The water-bearing rocks are thinly interbedded clay and carbonate sediments, with cracked-porous layers distributed randomly in lateral and vertical dimensions among 30 to 200 m thick impermeable rocks. The

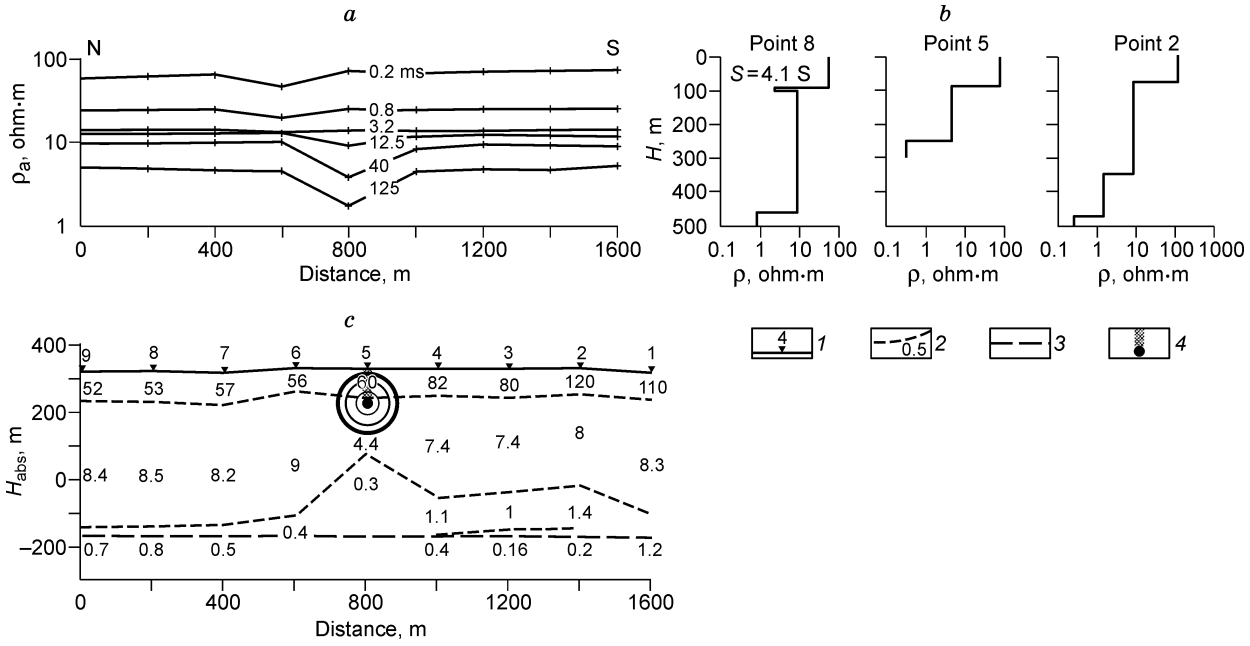

Fig. 4. Apparent resistivity (ρ_a) plots (*a*), results of 1D inversion (*b*), and 1D resistivity section (*c*) along N–S profile (see Fig. 1, *b* for profile location). *1*, TEM station and its number; *2*, resistivity interface and resistivity value in ohm · m; *3*, surface of Middle Cambrian aquifer; *4*, containment cavity and rubble chimney. Concentric circles of increasing radiuses correspond to crushed and cracked zones.

plane-bedded and monoclinal sediment sequences contain several aquifers. The groundwater pressure head is from 10 m (in the north) to 140–280 m (in the south) above the aquifer surface and the groundwater table is at +150 to +280 m asl. TDS is from 31 to 252 g/l in (90.5 g/l on average).

The resistivity of water-bearing porous rocks ρ_r is related to their porosity k_p (in fractions of 1) and the resistivity ρ_w of saturating water (Archie's law) as (Dobrynin et al., 1991; Kobranova, 1986):

$$\rho_r = a\frac{\rho_w}{k_p^m}, \qquad (2)$$

where $a \approx 1$; m (cementation factor) is a constant which is found empirically and known to be $m \approx 2$ in tightly cemented

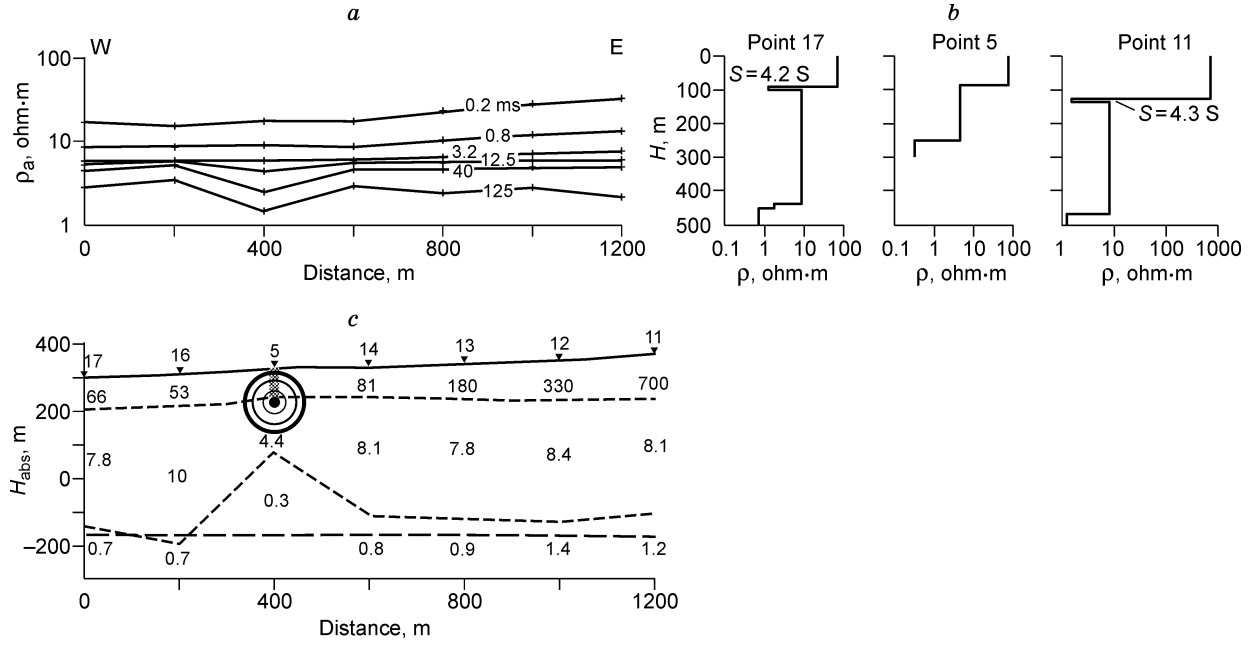

Fig. 5. Apparent resistivity (ρ_a) plots (*a*), results of 1D inversion (*b*), and 1D resistivity section (*c*) along W–E profile. See Fig. 1, *b* for profile location and Fig. 4 for legend.

terrigenous and carbonate rocks with intergranular porosity. Equation (2) implies the pore water resistivity ρ_w = 0.05–0.1 ohm · m if the porosity of carbonates in the second layer (ρ_2 = 5–10 ohm · m) is assumed to be k_p = 0.1. TDS (normalized to NaCl) in waters of this resistivity at about 0 °C is at least 150 g/l. At k_p = 0.2, the pore water will have the resistivity ρ_w = 0.2–0.4 ohm · m and, correspondingly, TDS = 30–60 g/l. These estimates are generally consistent with water chemistry data from boreholes.

As for the conducting basement, its surface is proximal to or almost coincides with the top of the Middle Cambrian aquifer within the lowermost Upper Cambrian Chukuk Formation clay-carbonate and Middle Cambrian carbonate sediments (Figs. 4, *c*, 5, *c*). The water-bearing section is confined from above by impermeable dense carbonate and clay of the Upper Cambrian Markha Formation. It includes three separate aquifers of different porosity types and fluid-dynamic patterns. TEM data resolve only the upper one and sometimes also the layer below it. The upper aquifer, porous-type, corresponds to the Chukuk Formation consisting of interbedded clayey limestone, limestone, and dolomite, with clay content no more than 20%. It has a laterally uniform thickness 90 m on average; the surface lies horizontally and is stripped at depths from 160 to 185 m below sealevel. The second aquifer is cavernous-porous and corresponds to a lagoonal dolomite sequence in the Middle Cambrian upper member. Its surface is at depths from –250 to –275 m asl and the thickness varies from 10 to 450 m being controlled by the position of bioherms at the base.

The resistivity ρ_3 of the conductive basement ranges from 0.2 to 1.4 ohm · m along profile 1 and from 0.7 to 1.4 ohm along profile 2 (Figs. 4, *c*, 5, *c*). With the existing groundwater setting of the area, the low resistivity of rocks may be due to saturation with saline waters. However, there arises a problem: Archie's law implies the resistivities of water $\rho_w = 2 \times 10^{-3}$ to 1.5×10^{-2} ohm · m at k_p = 0.1 and from 8×10^{-3} to 6×10^{-2} ohm · m at k_p = 0.2, with the assumed a = 1 and m = 2. These low resistivities are inconsistent with chloride pore fluids of any high salinity.

The fit between the inversion results and the petrophysical model can be improved by correcting the cementation factor m in (2), which is known to be $m \to 1$ in dense cemented rocks with cracks or other "direct" conduction paths, i.e., much less than m = 2 common to unfractured rocks (Dobrynin et al., 1991). At m = 1 we obtain a higher but still too low water resistivity: ρ_w = 0.02–0.14 ohm · m at k_p = 0.1 while a reasonable fit requires it to be at least 0.05 ohm · m at temperatures below 0 °C, even at TDS (NaCl) of the order of hundreds of g/l. For ρ_r to be 0.2 ohm · m at ρ_w = 0.05 ohm · m and m = 2, the porosity should be k_p = 0.5, which is unlikely in carbonate rocks. At m = 1 the porosity required to fit ρ_p = 0.2 ohm · m, is k = 0.25, which is a high but acceptable value (Dobrynin et al., 1991; Kobranova, 1986). The fact that the exponent m has to approach unity for reasonable interpretation of TEM data is implicit evidence that the Middle Cambrian aquifer must be of cracked-porous type.

Thus, the TEM surveys reveal no regional resistivity anomalies which would be a consequence of the underground nuclear explosion, i.e., the latter has caused no marked change to the position of aquifers. This inference agrees with evidence from studies of UNE effects on groundwater circulation: the groundwater table returns to the original level in about a year after explosions (Gorbunova and Spivak, 1997).

What may be then the cause of the local resistivity low (at t > 10 ms) measured at the UNE epicenter? According to engineering-geological and geophysical studies, contained nuclear explosions produce several distinct zones in the surrounding rocks (Adushkin and Spivak, 2004):

– containment (melt) cavity, with the radius R_{cav} = (10–13.6) · $Q^{1/3}$;

– sheared zone, with the thickness d_{shear} = (3–4) · $Q^{1/3}$;

– crushed zone, with the radius R_{crush} = (24–34) · $Q^{1/3}$;

– cracked zone (dense cracks), with the radius R_{crack} = (50–55) · $Q^{1/3}$;

– cracked zone (rare cracks, blocks), with the radius R_{block} = (65–75) · $Q^{1/3}$,

where Q is the charge in kiloton and all sizes are in meters. In addition to cracked zones around the containment cavity, there forms a rubble chimney above it which may reach the ground surface if the charge is detonated at shallow depths. Given that the "Crystal" explosion was 2 kt, the sizes of the zones must be (Figs. 4, *c*, 5*c*): R_{cav} = 13–17 m; d_{shear} = 4–5 m; R_{crush} = 30–40 m; R_{crack} = 60–70 m; R_{block} = 82–95 m.

As we wrote above in the *Results* section, the resistivity anomaly at the UNE site appears as a swelling surface of the conducting lower layer, with an uplift at least 200 m. The gained experience of TEM surveys for mineral and kimberlite exploration, as well as physical modeling (Vakhromeev and Kozhevnikov, 1988), indicate that the effect of a local conductor embedded in a layered earth shows up as uplift of conducting layers. Note that the inferred depth to the uplift above the local conductor and in its immediate vicinity is apparent rather than actual and is commonly greater than the true depth to the conducting object. Currently there is a possibility to model the 3D structure of the subsurface, including the UNE area, using 3D forward models (Trigubovich et al., 2009). Yet, appropriate 3D forward modeling and, more so, the subsequent inversion require a dense observation network, better with 2D arrays sampling three components of the induced magnetic field. The work reported here was, however, a reconnaissance and of a limited volume.

The idea that the anomaly at the UNE epicenter may be produced by a local conductor is consistent with the measured data. The anomalous TEM response was estimated by subtracting the background signal (a mean over all data points except the anomalous one) from that measured at the UNE epicenter (Fig. 6).

The difference transient looks like a straight line on the log scale at late times ($t \geq 40$ ms) and is thus a decreasing exponent, which is a typical of the transient process in a local conductor (Kaufman, 1971). The dashed line in Fig. 6, *a*, *b* shows the best fitting exponential decay to approximate the

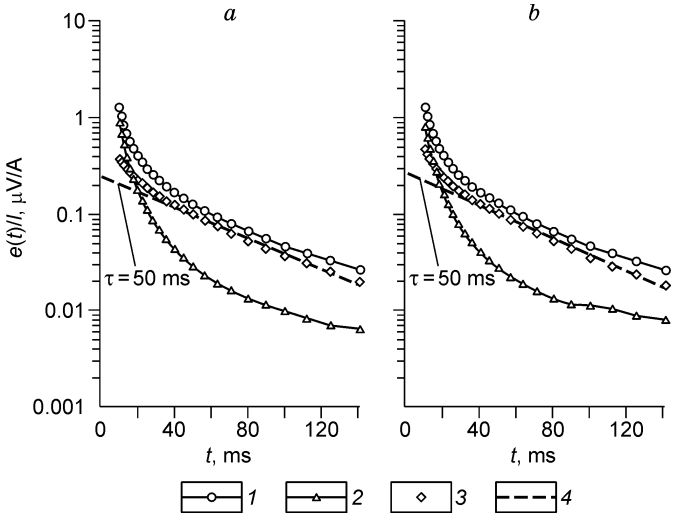

Fig. 6. Transient responses measured on N–S (*a*) and W–E (*b*) profiles. *1*, measured at UNE epicenter; *2*, background (average over all points except that of the UNE epicenter); *3*, anomalous transient found as difference between voltages measured at UNE epicenter and that of background; *4*, an exponent approximating the anomalous signal at late times.

anomalous signal in the interval from 40 to 140 ms. The estimated time constant τ is 50 ms.

In the context of this study, the local conductor can be reasonably approximated by a conducting sphere with the radius $r = R_{\text{block}}$ and the conductivity σ. The center of the sphere coincides with that of the containment cavity and the surrounding deformed zones, i.e., is at a depth of 100 m. At late times, vortex current in the conducting sphere decreases exponentially with time constant $\tau = \mu\sigma r^2/\pi^2$, where μ is absolute magnetic permeability of the sphere (Kaufman, 1971).

Given that $\mu = \mu_0 = 4\pi \times 10^{-7}$ H/m and $r \approx R_{\text{block}}$ = 90 m, the effective electrical conductivity (σ) of the sphere is 50 S/m and its resistivity is $\rho = 1/\sigma = 0.02$ ohm · m, which is very low and is hard to explain. One would obtain a more realistic value $\rho \geq 0.2$ ohm · m assuming the radius of the sphere to be 270 m or more instead of 90 m, but this contradicts the detonation depth of 100 m.

At the time given, one may only hypothesize that the cavity and the surrounding deformed rocks became low resistive because of very saline pore fluids, and for this reason appear as a local conductivity anomaly. However, the σ value is too high to be explainable within the limits of a reasonable petrophysical model. Another problem is where the water of this extremely high salinity may have come from?

The zone of deformed rocks, including the spherical cavity and the rubble chimney, is in the depth interval from 140–330 m on the 1D resistivity sections. The same interval covers the subpermafrost Upper Cambrian aquifer with brackish and saline waters of 30 to 250 g/l TDS (90 g/l on average). It appears very unlikely that saturation with waters of such a salinity could reduce the resistivity of the deformed rocks to 0.05 ohm · m taking into account the known respective resistivity of chloride waters (0.1–0.5 ohm · m). There is a more preferable candidate, namely, strong and very strong brines in the Middle Cambrian subpermafrost aquifer with its top at –165 to –185 m asl (Figs. 4, *c*, 5, *c*). Inasmuch as the pressure head of this water is at 310–350 m above the table (Alekseev, 2009), it may have risen to the UNE level provided that there existed a vertical permeable zone of deformed rocks between –170 and 140 m asl. However, this scenario is unlikely as such a zone can form only above the containment cavity as a result of collapse.

On the other hand, there is gamma spectrometry evidence (Golubov et al., 2004) from the lower section of the Udachny open pit (–125 m asl),—where groundwater drains the fractured northeastern pit wall,—that radon and thoron fissure products are in concentrations times greater than away from the groundwater discharge site. This is exactly the level where there lie the surface of the Middle Cambrian aquifer and the corresponding conductive basement mapped with the TEM soundings (Figs. 4, *c*, 5, *c*). Therefore, permeable paths may exist yet between the spherical zone of deformed rocks around the containment cavity and the Middle Cambrian aquifers below.

The resistivity pattern of the shallow subsurface is worth of a special comment. According to TEM data, the base of the upper layer is a continuous horizontal boundary and there are no anomalies within the layer (Figs. 5, 6). Therefore, the geoelectric parameters experienced no significant change, including at the UNE epicenter. This is an unexpected result because the effect of collapse in the chimney would be to deform and loosen shallow rocks and make them permeable for fluids and, correspondingly, less resistive (Stognii, 2004). The chimney, especially its periphery, are known to be permeable for fluids (Busygin et al., 1999). The air filtered through these zones must be warm, as the air temperature in containment cavities remains 30–50 °C even 10–15 years after UNE tests, i.e., these cavities act as long-term heat storage.

Conclusions

The background resistivity pattern at the “Crystal” UNE site corresponds to a three- or four-layer earth model with a conductive base. The uppermost layer, with a resistivity of tens to hundreds of ohm · m, has its bottom at 190–260 m asl and consists of perennially frozen Late Cambrian carbonates. The second layer has its bottom at 20 to 190 m below the sealevel and the resistivity 7–10 ohm · m. It is composed of frost-bound and unfrozen rocks that belong to an Upper Cambrian water-bearing sequence (aquifer unit). The third and fourth layers make up a conductive base of the section (0.2–1.4 ohm · m) the top of which matches the table of a Middle Cambrian aquifer. Although the water of this aquifer has very high TDS (up tp 400 g/l), explaining the extremely low resistivity requires a cracked-porous formation with porosity at least 0.25.

The anomalous transient response measured at the explosion site indicatse the presence of a local conductor possibly produced by highly saline waters in the containment cavity and in deformed rocks around it. However, the resistivity is too low (0.02 ohm · m) to be accounted for by any petrophysical model available at the present state of knowledge.

Another problem is to understand how the brines circulating at large depths may have reached the containment cavity and the surrounding rocks. Furthermore, it is unclear why the resistivity distribution in the upper section at the blast epicenter remained unperturbed though it was subject to strong mechanic and thermal effects.

The amount of data collected during the reported study of 2008 is insufficient to model the detailed resistivity distribution at the site; nevertheless, it has provided a first idea of the background TEM pattern and its UNE-induced changes.

It will be reasonable to continue the work and to set up more detailed surveys, possibly, jointly by TEM and MT methods, with 3D forward modeling, in order to improve the model of the UNE site and to resolve the arising problems. New knowledge will be also useful to estimate the applicability of electromagnetic methods to environment monitoring at the site and elsewhere in areas of underground nuclear blasting in Yakutia.

The study was run at the Sobolev Institute of Geology and Mineralogy, Novosibirsk, in 2008 through 2009, with participation of researchers from Institute of Petroleum Geology and Geophysics and from the *Luch* R&D Company, a manufacturer of geophysical instruments. The study was carried out as government contract No. 43 (76-08) with support from the Department of Radiation Safety of the Ministry of Nature Conservation, Sakha Republic (Yakutia).

The manuscript profited much from constructive criticism by G.M. Trigubovich.

References

Adushkin, V.V., Spivak, A.A., 2004. Effects of underground nuclear explosions on rock properties. Fizika Goreniya i Vzryva 40 (6), 15–24.

Alekseev, S.V., 2009. Permafrost-Groundwater Systems of the Yakutian Diamond Province [in Russian]. GEO Publishers, Novosibirsk.

Artamonova, S.Yu., Razvorotneva, L.I., Bondareva, L.G., Kozhevnikov, N.O., Antonov, E.Yu., Sobakin, P.I., Olesov, S.N., 2009a. Environment consequences of peaceful underground nuclear explosions in Yakutia, in: Radioactivity and Radioactive Elements in the Human Environment. Proc. III Int. Conf., Tomsk, 23–27 June 2009, STT, Tomsk, pp. 66–68.

Artamonova, S.Yu., Razvorotneva, L.I., Bondareva, L.G., Sobakin, P.I., Kozhevnikov, N.O., Antonov, E.Yu., Olesov, S.N., 2009b. Environment consequences of peaceful underground nuclear explosions: examples from "Crystal" and "Craton-3" sites. Proc. VI Russian Workshop, Conf. "Radiochemistry-2009", Moscow, 12–16 October 2009, FGUP "PO Mayak", Ozersk, p. 313.

Burtsev, I.S., Stepanova, S.K., Kolodeznikova, E.N., Arkhipov, A.D., 2004. Experience of exploring underground nuclear explosions and dumps of uraniferous ore in Yakutia, in: Radiation Safety of Sakha Republic (Yakutia). Proc. II Republican R&D Conf., YaFGU, Izd. SO RAN, Yakutsk, pp. 56–67.

Busygin, V.P., Andreev, A.I., Kosolapov, S.A., 1999. The thermal regime of the ground surface at epicenters of underground nuclear explosions. Izv. RAN, Fizika Zemli, No. 11, 68–74.

Dobrynin, V.M., Vendelshtein, B.Yu., Kozhevnikov, D.A., 1991. Petrophysics [in Russian]. Nedra, Moscow.

Drozdov, A.V., 2006. The structural-tectonical criteria for the assessment of injectivity of massives for the diamond-mining waste water disposal in the cryolithozone of Western Yakutia. Kriosfera Zemli X (2), 27–45.

Golubov, B.N., Sapozhnikov, Yu.A., Goralchuk, A.V., 2004. Migration of radionuclides from the cùntainmeòt cavity of the "Crystal" underground nuclear explosion into the Udachny diamond mine, in: Radiation Safety of Sakha Republic (Yakutia). Proc. II Republican R&D Conf., YaFGU, Izd. SO RAN, Yakutsk, pp. 182–192.

Gorbunova, E.M., Spivak, A.A., 1997. Changes in groundwater circulation caused by underground nuclear explosions. Geoekologiya, No. 6, 29–37.

Kaufman, A.A. (Ed.), 1971. Near-Field TEM Surveys [in Russian]. Preprint, SO AN SSSR, IGiG, Novosibirsk.

Kaufman, A.A., Morozova, G.M., 1970. Near-field TEM Surveys: Theoretical Background [in Russian]. Nauka, Novosibirsk.

Klimovskii, I.V., Gotovtsev, S.P., 1994. The Permafrost Zone of the Yakutian Diamond Province [in Russian]. Nauka, Novosibirsk.

Klimovskii, I.V., Gotovtsev, S.P., Shepelev, V.V., 2002. Groundwater and permafrost settings at the site of underground disposal of drainage water in Udachnaya kimberlite pipe. Kriosfera Zemli VI (3), 45–50.

Kobranova, V.N., 1986. Petrophysics [in Russian]. Nedra, Moscow.

Kozhevnikov, N.O., Plotnikov, A.E., 2004. Estimating the potentialities of the TEM method for studying shallow ground. Geofizika, No. 6, 33–38.

Matveev, B.K., 1974. Interpretation of TEM Data [in Russian]. Nedra, Moscow.

Mel'nikov, V.P., Oberman, N.G., Velizhanina, I.A., Davidenko, N.M., 2000. Influence of underground nuclear explosions on natural environment of the North. Geologiya i Geofizika (Russian Geology and Geophysics) 41 (2), 280–291 (281–293).

Mikulenko, K.I., Chomchoev, A.I., Burtsev, I.S., 2004. Regional geological stability zoning of the Yakutia territory, in: Radiation Safety of Sakha Republic (Yakutia). Proc. II Republican R&D Conf., YaFGU, Izd. SO RAN, Yakutsk, pp. 67–75.

Mikulenko, K.I., Chomchoev, A.I., Gotovtsev, S.P., 2006. Underground Nuclear Explosions in the Territory of Sakha Republic (Yakutia): Geological and Geophysical Setting and Consequences [in Russian]. Izd. YaNTs SO RAN, Yakutsk.

Rabinovich, B.I., 1987. Fundamentals of Near-Field TEM Surveys [in Russian]. IPI, Irkutsk.

Stognii, V.V., 2004. Local geophysical monitoring at sites of underground nuclear explosions in Yakutia, in: Radiation Safety of Sakha Republic (Yakutia). Proc. II Republican R&D Conf., YaFGU, Izd. SO RAN, Yakutsk, pp. 252–260.

Trigubovich, G.M., Persova, M.G., Soloveichik, Yu.G., 2009. 3D TEM-TDEM Surveys [in Russian]. Nauka, Novosibirsk.

Vakhromeev, G.S., Kozhevnikov, N.O., 1988. Methods of TEM Soundings for Mineral Exploration [in Russian]. Irkutsk University Press, Irkutsk.

Vanchugov, V.A., Kozhevnikov, N.O., 1998. Methods and results of TEM soundings for the resistivity structure of the Nakyn kimberlite field (Western Yakutiya), in: Uchitel, M.S. (Ed.), Geology, Prospecting and Exploration of Mineral Deposits. Collection of Papers [in Russian] (Transactions of Irkutsk Technological University, Issue 22). Irkutsk Technological University, Irkutsk, pp. 164–176.

Yablokov, A.V., 2009. "A stout monster, wild, huge, hundred-mawed, and barking": An Environmentalist about Nuclear Industry [in Russian]. Publication of the Baikal Environment Conservation Movement *Volna* ("Wave"), Irkutsk.

Editorial responsibility: M.I. Epov